Network Modeling of an Inclined and Off-Center Microstrip-Fed Slot Antenna

Jeong Phill Kim, *Member, IEEE*, and Wee Sang Park, *Member, IEEE*

***Abstract*—This paper describes a general method for analyzing a microstrip-fed slot antenna with a view to developing an improved network model featuring an inclined and off-center slot. The network model consists of an ideal transformer, a radiation conductance, and extended slotlines terminated by short circuit. The transformer turn ratio can be calculated by combining the reciprocity theorem with the spectral-domain immittance approach. The radiation conductance is determined by the radiated power from the slot in the forms of space and surface waves in the spectral domain. Then network models corresponding to several variations of the antenna are described and the series impedances are computed. The computed results using the network model are compared with the rigorous solution and measurements and good agreements are obtained.**

***Index Terms*— Circuit modeling, microstrip antennas, reciprocity theorem, slot antennas, spectral domain analysis.**

I. Introduction

RECENTLY, interest has increased in the monolithic integration of microstrip antennas and circuitry for phased array radars, wireless communications, and related applications. A microstrip-fed slot antenna, where a rectangular slot is cut in the ground plane of a microstrip line [1], is one promising candidate for the radiators for these applications [2], [3].

When a microstrip-fed slot antenna is designed with available substrate materials and a thickness such that the microstrip line crosses the center of the slot orthogonally, the radiation resistance becomes much higher than the characteristic impedance of the microstrip line. To better match the rest of the circuit, the radiation resistance should be reduced, and there are three possible ways to accomplish that. The first one is off-center feeding suggested by Yoshimura [1], where the feed point is moved away from the center of the slot. The second one is truncating one side of the microstrip line and loading the termination by an open-circuit tuning stub [4], which changes the resonant frequency of the slot. The third possibility is inclining the axis of the slot, so it is no longer orthogonal to the microstrip line. This paper discusses the first and third alternatives.

In the past, problems related to the microstrip-fed slot antenna have undergone some analysis. The concept of complex radiated power and modal voltage discontinuity with some approximations has been applied to obtain the input impedance [5]. Recently, full-wave rigorous analyzes [4], [6], [7] have also been done successfully, but these approaches require excessive computation and do not provide conceptual insight into the circuit. Some approximate network models have been proposed to design the antenna efficiently. Axelrod *et al.* [8] explained the radiation characteristics of the slot by an experimentally determined resistance and modeled the microstrip-slotline junction by employing an ideal transformer with the turn ratio given by Knorr [9]. Himdi *et al.* [10] used a lossy transmission line model to determine the attenuation constant and radiation conductance of the slot. Akhavan *et al.* [11] evaluated the radiation conductance by using the standard expression for the resonant slot without substrate, and determined the self and mutual inductances of the transformer approximately. These modeling schemes, however, are restricted to off-center orthogonal slot antennas. The resonant frequency of an off-center slot antenna will undergo some change as the offset distance varies. Himdi *et al.* [10] showed that the resonant frequency remains constant, whereas the rigorous solution [12] indicates that it decreases. Our model also reveals a decrease in resonant frequency.

This paper is intended to present a method for analyzing the microstrip-fed slot antenna in order to develop an improved equivalent network model which can accommodate an inclined and off-center slot. The model is a two-port network consisting of an ideal transformer, a radiation conductance, and extended slotlines terminated by short circuit. Analytical expressions for the turn ratio of the ideal transformer and the radiation conductance are derived in Section II. In Section III, the proposed model is applied to various types of the antenna, and the results are compared with measured as well as computed findings from previous theories and the rigorous solution. Our conclusions are given in Section IV.

II. Analysis Method

A. Formulation

Fig. 1 shows a scheme of the microstrip-fed slot antenna. The slot is arbitrarily inclined to the microstrip line at an angle θ_s and has an offset distance d from the center in the direction of the slot axis. L_s and W_s denote the length and width of the slot. The substrate has a dielectric constant ϵ_r and a thickness h. The width of the microstrip line is W_m.

An incident field is first launched from $x = -\infty$ into port 1 and propagates to port 2 with the slot absent. The scattered

Manuscript received July 22, 1997; revised January 12, 1998.

J. P. Kim is with the Research and Development Center, Precision Co., Ltd., Yongin, Kyunggi-Do 449-910, Korea.

W. S. Park is with the Department of Electronic and Electrical Engineering, Pohang University of Science and Technology, Pohang, Kyungbuk 790-784, Korea.

Publisher Item Identifier S 0018-926X(98)06100-6.

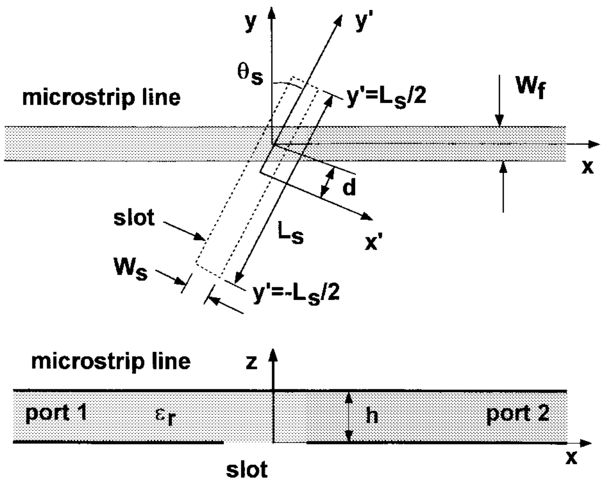

Fig. 1. Top and side views of a microstrip-fed slot antenna.

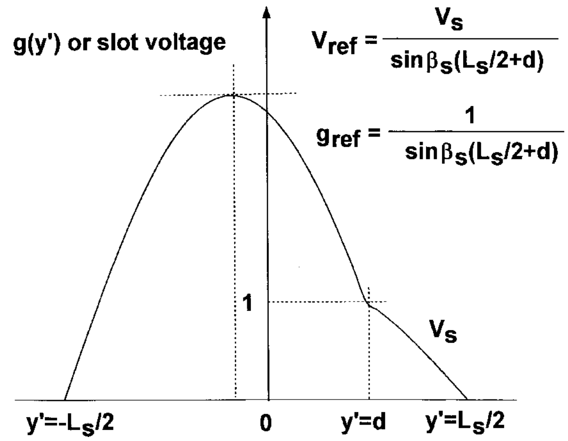

Fig. 2. Chosen electric field and slot voltage distributions along the slot axis.

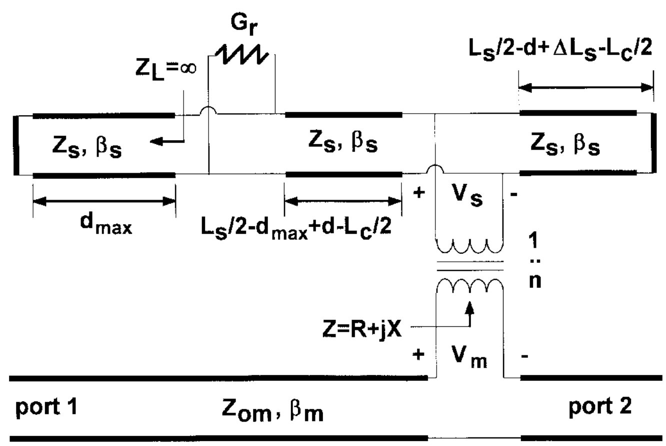

Fig. 3. Equivalent network model of a microstrip-fed slot antenna.

field generated by the slot on the ground plane exists on both port 1 and port 2. Since the total electromagnetic field can be expressed as the sum of the incident and scattered fields, the magnetic field $\overline{H}$ is expressed as

$$\overline{H} = \begin{cases} \overline{h}^{+} e^{-j\beta_m x} + \Gamma_1 \overline{h}^{-} e^{j\beta_m x}, & \text{for } x \le 0 \\ (1+\Gamma_2)\overline{h}^{+} e^{-j\beta_m x}, & \text{for } x \ge 0 \end{cases} \tag{1}$$

where β_m is the phase constant of the dominant mode of the microstrip line. The electric field $\overline{E}$ is similarly given when $\overline{h}$ is replaced by $\overline{e}$ in (1). The field eigenvectors of the microstrip line, $\overline{e}^{+}$ and $\overline{h}^{+}$, are normalized such that

$$\iint_{S_m} (\overline{e}^{+} \times \overline{h}^{+}) \cdot \hat{x} \, dy \, dz = 1 \tag{2}$$

where S_m is the cross section of the microstrip line. $\overline{e}^{-}$ and $\overline{h}^{-}$ are also similarly normalized. Γ_1 and Γ_2 in (1) represent quantities related to the scattered field due to the induced voltage across the slot, and Γ_1 and $(1+\Gamma_2)$ become the reflection and transmission coefficients, respectively.

For a narrow rectangular slot, the induced electric field $\overline{E}_s$ for the voltage V_s across the slot at the feed point can be represented as $\overline{E}_s = -\hat{x}' V_s \, e_s$ with

$$e_s = \frac{1}{\pi\sqrt{(W_s/2)^2 - x'^2}} \, g(y'). \tag{3}$$

$g(y')$ in (3) indicates the field variation along the slot axis and is chosen as an asymmetric piecewise-sinusoid (PWS) mode (as shown in Fig. 2)

$$g(y') = \frac{\sin\beta_s(y' \pm L_s/2)}{\sin\beta_s(d \pm L_s/2)} \tag{4}$$

where the $+$ and $-$ signs in front of $L_s/2$ correspond to the cases for $-L_s/2 < y' < d$ and $d < y' < L_s/2$, respectively.

Invoking the reciprocity relation [4], [13] with some algebraic manipulations produces $\Gamma_i/V_s (i = 1, 2)$ as

$$\frac{\Gamma_i}{V_s} = \frac{-1}{2} \iint_{S_s} (-\hat{x}' e_s \times \overline{h}_i) \cdot \hat{z} \, dS \tag{5}$$

with $\overline{h}_1 = \overline{h}^{+} e^{-j\beta_m x}$ and $\overline{h}_2 = \overline{h}^{-} e^{j\beta_m x}$, where S_s is the entire slot opening on the ground plane.

B. Equivalent Circuit

The microstrip-fed slot antenna can be viewed as a microstrip line discontinuity and represented by an equivalent two-port network as shown in Fig. 3. The slot antenna is modeled as a series load. The voltage discontinuity ΔV_m on the microstrip line due to the slot can be represented as $\Delta V_m = (\Gamma_1 - \Gamma_2)V_m$ for the line voltage V_m, and the magnitude of V_m equals $\sqrt{Z_{om}}$ under the normalization of (2). Z_{om} is the characteristic impedance of the microstrip line. Therefore, the turn ratio n defined as $\Delta V_m/V_s$ in Fig. 3 can be obtained by using (5) and performing vector operations as

$$n = \frac{\sqrt{Z_{om}}}{2} \left[(n_{x1} - n_{x2}) \sin\theta_s + (n_{y1} + n_{y2}) \cos\theta_s\right] \tag{6}$$

where

$$n_{x1} = \iint_{S_s} e_s \, h_x \, e^{-j\beta_m x} \, dS$$
$$n_{y1} = \iint_{S_s} e_s \, h_y \, e^{-j\beta_m x} \, dS. \tag{7}$$

In (7), h_x and h_y denote the x- and y-components of the magnetic field eigenvector $\overline{h}^{+}$. n_{x2} and n_{y2} in (6) take similar values to n_{x1} and n_{y1}, respectively, except for the opposite sign of β_m. Evaluations of n_{x1} and n_{y1} are detailed in the Appendix.

Next, the slot is considered as a radiation conductance and two short-circuit slotlines with characteristic impedance Z_s and phase constant β_s. The reference position of the radiation conductance is set at $y' = -L_s/2 + d_{\max}$ instead of the feed position, where $d_{\max}$ denotes the distance from the end to the first maximum of the electric field of a semi-infinite slotline. This choice enables us to neglect the left section of the slotline and prevents the slot admittance from being infinite even for a zero electric field at the feed point.

For the reference voltage V_{ref} given as $V_s/\sin\beta_s(L_s/2+d)$ in Fig. 3, the radiation conductance G_r of the slot is defined as

$$G_r = \frac{P_{rd} + P_{ra} + P_{sur}}{2\,\mathrm{V}_{ref}^2} \tag{8}$$

where P_{rd} and P_{ra} are the radiated powers from the slot into the substrate and air sides, respectively, in the form of space wave, and P_{sur} is the power carried by the surface wave which exists in the dielectric substrate.

With the help of the reaction formula and Parseval's theorem [14], P_{rd} can be expressed as

$$P_{rd} = \mathrm{Re}\left[\iint_{S_k} \frac{k_{x'}^2 \tilde{Y}_{\mathrm{TE}} + k_{y'}^2 \tilde{Y}_{\mathrm{TM}}}{8\pi^2(k_{x'}^2 + k_{y'}^2)} \left|\tilde{M}\right|^2 dk_{x'}\, dk_{y'}\right] \tag{9}$$

where S_k is the visible region $(k_{x'}^2 + k_{y'}^2 \le k_0^2)$. $k_{x'}$ and $k_{y'}$ are the wave numbers in the x'- and y'-directions, respectively, and k_0 is the wave number in free space. In (9), Re means taking the real part of the integral, and $\tilde{Y}_{\mathrm{TE}}$ [15], the admittance parameter of the TE_z mode for the substrate side, is given as

$$\tilde{Y}_{\mathrm{TE}} = Y_{od}^{\mathrm{TE}}\, \frac{Y_{oo}^{\mathrm{TE}} + Y_{od}^{\mathrm{TE}} \tanh(\gamma_{dz} h)}{Y_{od}^{\mathrm{TE}} + Y_{oo}^{\mathrm{TE}} \tanh(\gamma_{dz} h)} \tag{10}$$

where $Y_{oo}^{\mathrm{TE}} = \gamma_{oz}/j\omega\mu_o$, $Y_{od}^{\mathrm{TE}} = \gamma_{dz}/j\omega\mu_o$, $\gamma_{oz} = \sqrt{k_{x'}^2 + k_{y'}^2 - k_0^2}$, and $\gamma_{dz} = \sqrt{k_{x'}^2 + k_{y'}^2 - k_0^2\epsilon_r}$. The expression of $\tilde{Y}_{\mathrm{TM}}$ in (9) is the same as $\tilde{Y}_{\mathrm{TE}}$ with the related parameters for the TM_z mode: $Y_{oo}^{\mathrm{TM}} = j\omega\epsilon_o/\gamma_{oz}$ and $Y_{od}^{\mathrm{TM}} = j\omega\epsilon_o\epsilon_r/\gamma_{dz}$. $\tilde{M}$ in (9) is the Fourier transform of the equivalent magnetic current source $\overline{M} = \overline{E}_s \times \hat{z}$ on the slot opening. The integrand in (9) is well-behaved in the integration range and P_{rd} can be numerically integrated without difficulty. P_{ra} can be evaluated in a similar way with the admittance parameters for the air side. Using the singularity extraction technique [16] in the neighborhood of singular points associated with the surface wave modes, P_{sur} can be determined from the same integral as in (9). For an electrically thin substrate, its amount is usually small compared to the sum of P_{rd} and P_{ra}.

In the equivalent circuit shown in Fig. 3, ΔL_s is the extended slotline length due to the nonzero inductance at the end. A compensation length L_c is introduced to take into account the proximity effect of the microstrip line on the slot. One phenomenon of the effect is the increase of the resonant frequency of the slot. The factors affecting the compensation length include the microstrip line structure, the inclination angle, and the offset distance. Some physical consideration and comparisons of the present simulation with the rigorous solution with respect to the resonant frequency have led us to express L_c as

$$L_c = 2.0 \times 10^{-2}\, \frac{W_m}{h\sqrt{\epsilon_r}/\lambda_0}\, n^2 \sin\beta_s(L_s/2 + d). \tag{11}$$

III. Results and Discussions

To show the validity of the present theory, we shall determine n and G_r in the equivalent circuit. The slotline parameters Z_s, β_s, and ΔL_s can be calculated by using various analysis methods [17]. $d_{\max}$ can be determined from β_s and ΔL_s. L_c can also be determined by (11). Using these values, we can compute the series impedance of the equivalent circuit by using the general network theory [18]. The results are then compared with measured and computed data available in the literature.

We treat the antenna with an orthogonal and centered slot ($d = 0$ and $\theta_s = 0°$) first. The structure parameters are $W_m = 5$ mm, $h = 1.6$ mm, $\epsilon_r = 2.20$, $L_s = 40.2$ mm, and $W_s = 0.7$ mm. The slotline parameters, the turn ratio, and the radiation conductance are shown in Fig. 4(a) and (b) over the frequency range from 2 to 4 GHz. In Fig. 4(a), λ_0 and λ_s denote the free-space wavelength and the guide wavelength in the slotline, respectively. At $f = 3$ GHz, $d_{\max}$ becomes 19.77 mm and the radiation efficiency, which is defined by $(P_{rd} + P_{ra})/(P_{rd} + P_{ra} + P_{sur})$, is 0.94. It is found that if L is equal to $4W_m$ and $-7 \le m \le 7$, then the error of the turn ratio is less than 0.5%. As L increases, more summation terms are needed to obtain the same accuracy. Our computed results of the normalized series impedance are pictured in Fig. 4(c) along with the measured data reported by Himdi *et al.* [10], as well as the rigorous solution based on the method of moments [12]. The present theory agrees well with Himdi *et al.* and the rigorous solution. As is predicted, the slot resistance is much larger than the characteristic impedance of the microstrip line.

To further test the validity of the proposed network model, we can examine the antenna with an inclined slot ($\theta_s \ne 0°$). The structure parameters are the same as those in the circuit in Fig. 4 except for the inclination angle. Fig. 5(a) shows the turn ratio with respect to the inclination angle at $f = 3.2$ GHz; n decreases as θ_s increases. For the inclined slot, G_r is independent of the inclination angle. The results of the normalized series impedance for the different inclination angles over the frequency range from 2 to 4 GHz are shown in Fig. 5(b) and (c). The rigorous solution [12] is also presented for the purpose of comparison and it agrees well with the present theory. From Fig. 5(a) and (11), we note that as θ_s increases, L_c decreases, which induces the decrease of the resonant frequency of the slot toward its self-resonant frequency of 2.95 GHz as shown in Fig. 5(c).

Next, the present theory is applied to the antenna with an off-center slot ($d \ne 0$). The structure parameters are $W_m = 5$ mm, $h = 1.6$ mm, $\epsilon_r = 2.2$, $L_s = 60$ mm, $W_s = 2$ mm, and $\theta_s = 0°$. In Fig. 6(a) and (b), the computed results of the normalized series impedance are compared with the rigorous solution [12] for the different offset distances over the frequency range from 1.7 to 2.7 GHz. It is noted that as d increases, the resonant frequency decreases toward the

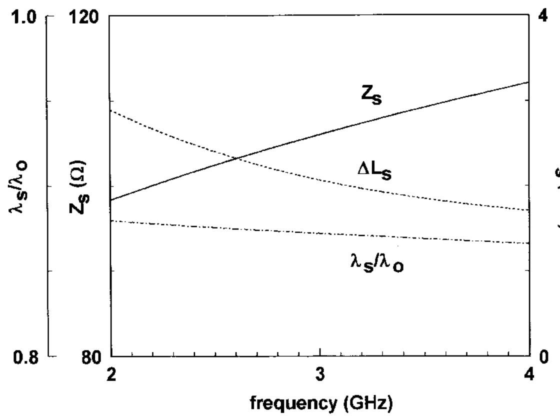

(a)

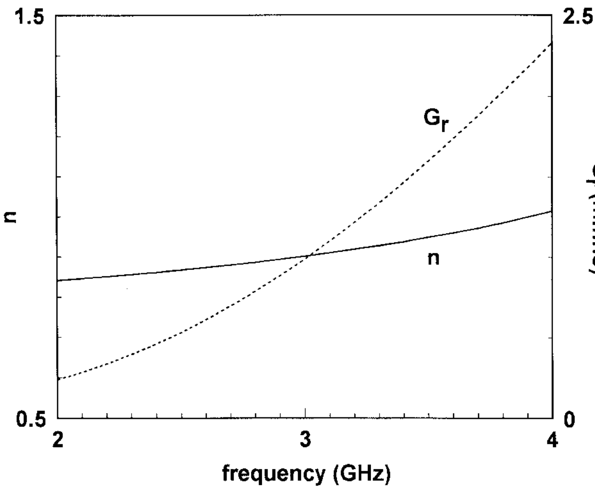

(b)

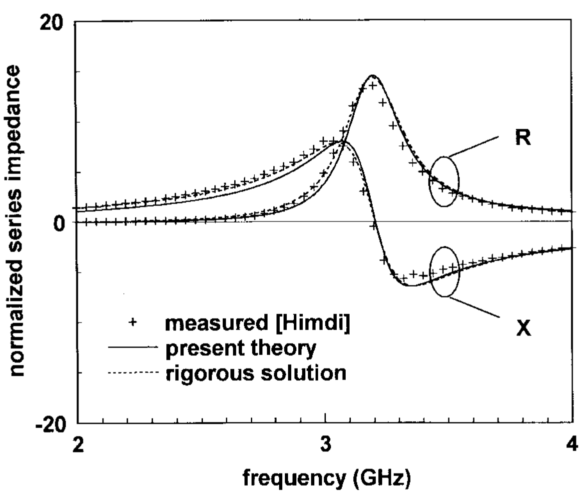

(c)

Fig. 4. Normalized series impedance of a microstrip-fed slot antenna ($W_m = 5$ mm, $h = 1.6$ mm, $\epsilon_r = 2.20$, $L_s = 40.2$ mm, $W_s = 0.7$ mm, $d = 0$ mm, $\theta_s = 0°$). (a) Characteristic impedance, normalized guide wavelength, and extended slotline length. (b) Turn ratio and radiation conductance. (c) Normalized series impedance.

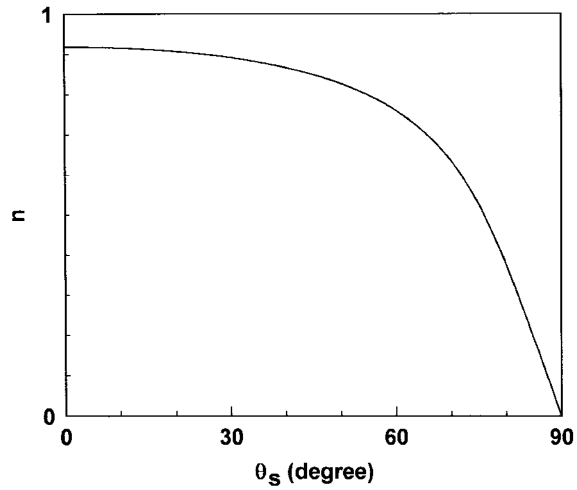

(a)

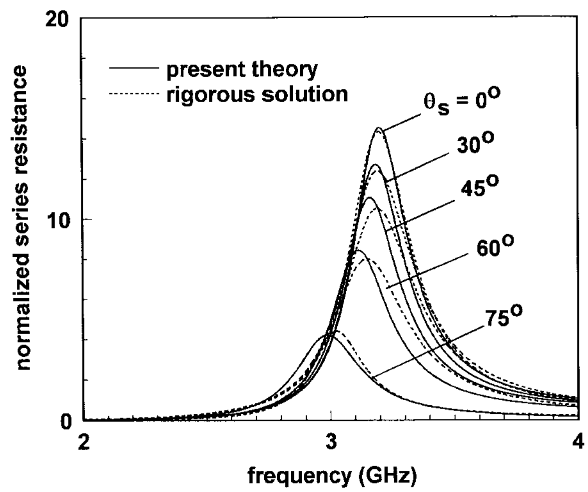

(b)

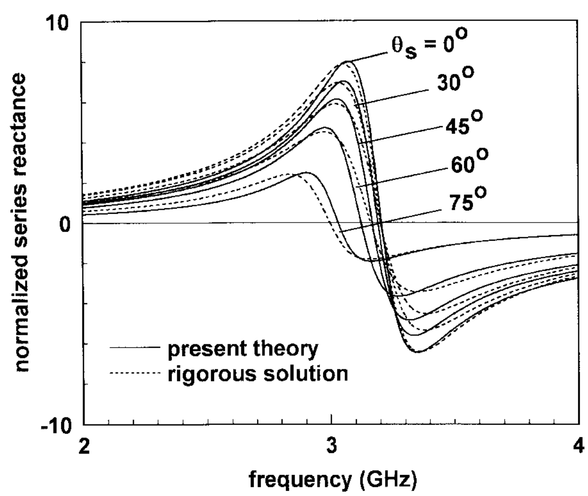

(c)

Fig. 5. Effect of the inclination angle of a slot on the normalized series impedance of a microstrip-fed slot antenna ($W_m = 5$ mm, $h = 1.6$ mm, $\epsilon_r = 2.20$, $L_s = 40.2$ mm, $W_s = 0.7$ mm, $d = 0$ mm). (a) Turn ratio with respect to inclination angle at $f = 3.2$ GHz. (b) Normalized series resistance. (c) Normalized series reactance.

self-resonant frequency of the slot. Again the result is a good agreement.

Finally, we fabricated two microstrip-fed slot antennas corresponding to the above two cases. One antenna has the inclination angle of 60°, and the length L_m of the microstrip open stub is 42.6 mm. The other antenna has the offset distance

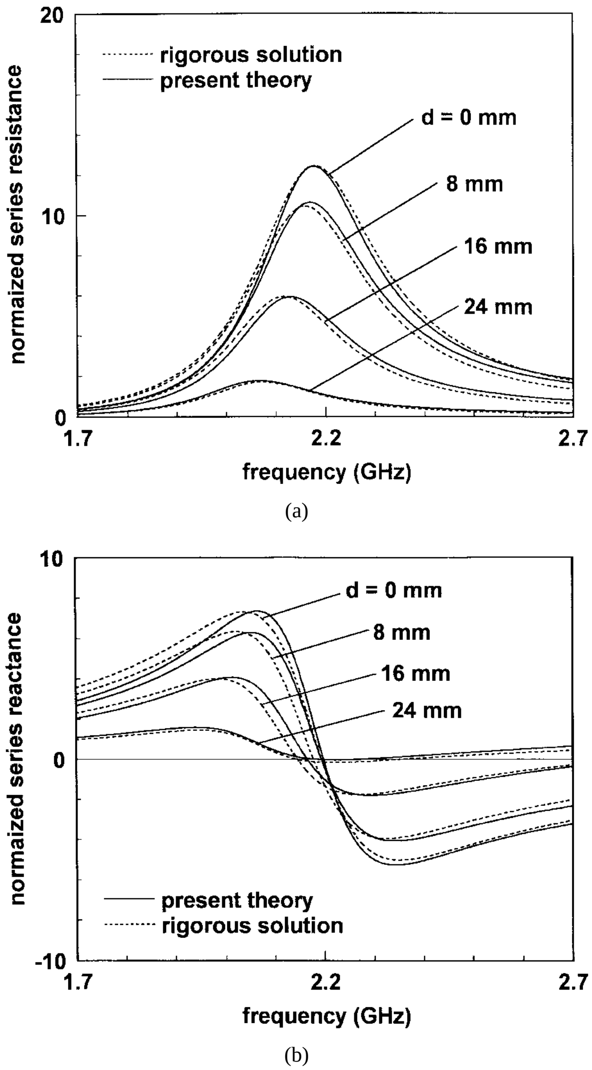

Fig. 6. Effect of the offset distance of a slot on the normalized series impedance of a microstrip-fed slot antenna ($W_m = 5$ mm, $h = 1.6$ mm, $\epsilon_r = 2.20$, $L_s = 60$ mm, $W_s = 2$ mm, $\theta_s = 0°$). (a) Normalized series resistance. (b) Normalized series reactance.

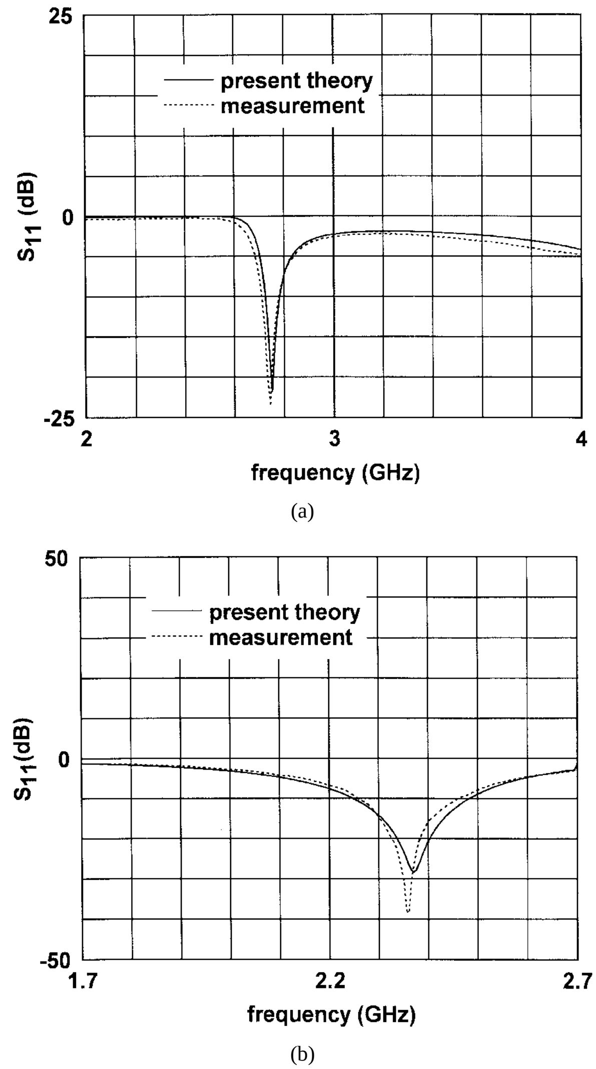

Fig. 7. Return loss for the microstrip-fed slot antennas (a) with an inclined slot ($W_m = 5$ mm, $h = 1.6$ mm, $\epsilon_r = 2.20$, $L_s = 40.2$ mm, $W_s = 0.7$ mm, $d = 0$ mm, $\theta_s = 60°$, $L_m = 42.6$ mm) and (b) with an off-center slot ($W_m = 5$ mm, $h = 1.6$ mm, $\epsilon_r = 2.20$, $L_s = 60$ mm, $W_s = 2$ mm, $d = 20$ mm, $\theta_s = 0°$, $L_m = 29.2$ mm).

of 20 mm with $L_m = 29.2$ mm. For a perfect impedance matching, L_m is chosen to cancel the series reactance of the antenna at the frequency where the normalized series resistance becomes unity. The measured results of the return loss are plotted in Fig. 7(a) and (b) along with the computed results by the present theory. It is clear that the agreements are good. All the results we obtained indicate the validity and accuracy of the present theory.

IV. Conclusion

This paper has proposed a general theory to analyze a microstrip-fed slot antenna with a view to developing an improved equivalent network model which can accommodate an inclined and off-center slot. The equivalent two-port network consists of an ideal transformer, a radiation conductance, and extended slotlines terminated by short circuit. The turn ratio was formulated explicitly in relation to the induced slot electric field and the magnetic field of the microstrip line by invoking the reciprocity theorem. For computational convenience and efficiency, a finite Fourier transform in conjunction with the spectral-domain immittance approach was used to evaluate the magnetic field on the ground plane of the microstrip line. The radiation conductance was determined from the self-reaction of the slot in the spectral domain. The series impedance of the equivalent circuit was calculated by the general network theory.

The present theory was applied to various models of the antenna. The results were in agreement with the measured data as well as the computed results from previous theories and the rigorous solution. Due to its simplicity and efficiency, the proposed network model is advantageous in analyzing and designing of a microstrip-fed slot antenna.

Appendix
Evaluation of n_{x1} and n_{y1}

Consider the microstrip line shown in Fig. 8, which is surrounded by the fictitious boundary walls at a large distance

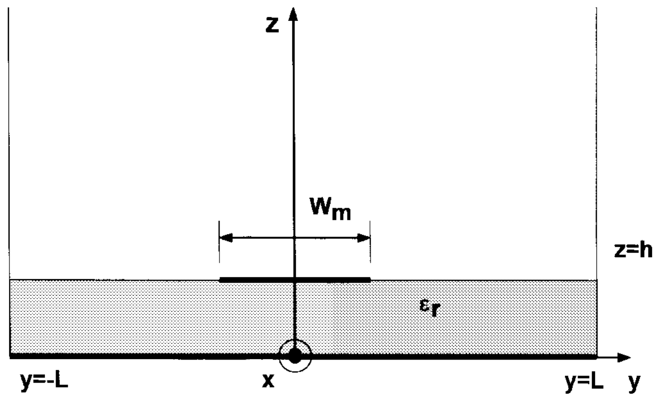

Fig. 8. Microstrip line with fictitious walls.

$y = \pm L$ so that the walls do not disturb the electromagnetic field distribution around the microstrip line. This situation enables us to use the finite Fourier transform $\tilde{h}_x$ of h_x instead of the infinite Fourier integral for the y-direction as

$$\tilde{h}_x(k_{ym}, z) = \int_{-L}^{L} h_x(y, z)\, e^{+jk_{ym}y}\, dy \tag{12}$$

$$h_x(y, z) = \frac{1}{4L} \sum_{m=-\infty}^{\infty} \tilde{h}_x(k_{ym}, z)\, e^{-jk_{ym}y} \tag{13}$$

with $k_{ym} = m\pi/(2L)$ and $m = 0, \pm 1, \pm 2, \cdots$. The expression for the finite Fourier transform pair $\tilde{h}_y$ and h_y can be obtained from (12) and (13) with h_x replaced by h_y. The source of h_x and h_y is the forward traveling current whose magnitude equals $1/\sqrt{Z_{om}}$. For a narrow strip, the surface current density can be approximated only as an x-component J_x with its Fourier transform $\tilde{J}_x$

$$J_x(y) = \frac{1}{\sqrt{Z_{om}}}\, \frac{1}{\pi\sqrt{(W_m/2)^2 - y^2}} \tag{14}$$

$$\tilde{J}_x(k_{ym}) = \frac{1}{\sqrt{Z_{om}}}\, J_0\left(\frac{W_m}{2}|k_{ym}|\right). \tag{15}$$

Using the spectral-domain immittance approach [15], $\tilde{h}_x$ and $\tilde{h}_y$ on the ground plane can be derived as

$$\tilde{h}_x(k_{ym}, 0) = \frac{1}{\cosh(\gamma_{dzm}h)}\, \frac{\beta_m k_{ym}}{\beta_m{}^2 + k_{ym}{}^2} \cdot \left[\frac{-Y_{\rm TM}^-}{Y_{\rm TM}^- + Y_{\rm TM}^+} + \frac{Y_{\rm TE}^-}{Y_{\rm TE}^- + Y_{\rm TE}^+}\right] \tilde{J}_x(k_{ym}) \tag{16}$$

$$\tilde{h}_y(k_{ym}, 0) = \frac{1}{\cosh(\gamma_{dzm}h)}\, \frac{1}{\beta_m{}^2 + k_{ym}{}^2} \cdot \left[\frac{\beta_m^2\, Y_{\rm TM}^-}{Y_{\rm TM}^- + Y_{\rm TM}^+} + \frac{k_{ym}^2\, Y_{\rm TE}^-}{Y_{\rm TE}^- + Y_{\rm TE}^+}\right] \tilde{J}_x(k_{ym}). \tag{17}$$

with the following admittance parameters [15]:

$$Y_{\rm TM}^+ = \frac{j\omega\epsilon_o}{\gamma_{ozm}}, \qquad Y_{\rm TM}^- = \frac{j\omega\epsilon_o\epsilon_r}{\gamma_{dzm}}\, \coth(\gamma_{dzm}h)$$
$$Y_{\rm TE}^+ = \frac{\gamma_{ozm}}{j\omega\mu_o}, \qquad Y_{\rm TE}^- = \frac{\gamma_{dzm}}{j\omega\mu_o}\, \coth(\gamma_{dzm}h) \tag{18}$$

where

$$\gamma_{ozm} = \sqrt{\beta_m^2 + k_{ym}^2 - k_o^2},$$
$$\gamma_{dzm} = \sqrt{\beta_m^2 + k_{ym}^2 - k_o^2\epsilon_r}. \tag{19}$$

When we substitute (3) and (13) into (7), and separate the integrals into x'- and y'-components, n_{x1} can be expressed as

$$n_{x1} = \frac{1}{4L} \sum_{m=-\infty}^{\infty} \tilde{h}_x(k_{ym}, 0)\, I_{x'1}(k_{ym})\, I_{y'1}(k_{ym}) \tag{20}$$

where $I_{x'1}(k_{ym})$ and $I_{y'1}(k_{ym})$ are

$$I_{x'1}(k_{ym}) = J_0\left(\frac{W_s}{2}\, |k_{ym}\, \sin\,\theta_s - \beta_m\, \cos\,\theta_s|\right) \tag{21}$$

$$I_{y'1}(k_{ym}) = \int_{-L_s/2}^{L_s/2} g(y')\, e^{-j(k_{ym}\,\cos\,\theta_s + \beta_m\,\sin\,\theta_s)(y'-d)}\, dy'. \tag{22}$$

The expression of n_{y1} can be obtained from (20) when $\tilde{h}_x(k_{ym}, 0)$ is replaced by $\tilde{h}_y(k_{ym}, 0)$.

REFERENCES

[1] Y. Yoshimura, “A microstrip-fed slot antenna,” *IEEE Trans. Microwave Theory Tech.*, vol. MTT-20, pp. 760–762, Nov. 1972.

[2] R. J. Mailloux, “Phased array architecture for mm-wave active arrays,” *Microwave J.*, vol. 29, pp. 117–124, July 1986.

[3] D. M. Pozar and D. H. Schaubert, “Comparison of architectures for monolithic phased array antennas,” *Microwave J.*, vol. 29, pp. 93–104, Mar. 1986.

[4] D. M. Pozar, “Reciprocity method of analysis for printed slot and slot-coupled microstrip antennas,” *IEEE Trans. Antennas Propagat.*, vol. AP-34, pp. 1439–1446, Dec. 1986.

[5] B. N. Das and K. K. Joshi, “Impedance of a radiating slot in the ground plane of a microstrip line,” *IEEE Trans. Antennas Propagat.*, vol. AP-30, pp. 922–926, May 1982.

[6] A. K. Bhattacharyya, Y. M. M. Antar, and A. Ittipiboon, “Full wave analysis for the equivalent circuit of an inclined slot on a microstrip ground plane,” *Proc. Inst. Elect. Eng.*, vol. 139, pt. H, no. 3, June 1992, pp. 245–250.

[7] C. Chen and N. G. Alexopoulos, “Modeling microstrip line fed slot antennas with arbitrary shape,” *Electromagn.*, vol. 15, no. 5, pp. 567–586, Sept./Oct. 1995.

[8] A. Axelrod, M. Kisliuk, and J. Moaz, “Broadband microstrip-fed slot radiator,” *Microwave J.*, pp. 81–94, June 1989.

[9] J. B. Knorr, “Slot-line transitions,” *IEEE Trans. Microwave Theory Tech.*, vol. MTT-22, pp. 548–554, May 1974.

[10] M. Himdi and J. P. Daniel, “Analysis of printed linear slot antenna using lossy transmission line model,” *Electron. Lett.*, vol. 28, no. 6, pp. 598–601, Mar. 1992.

[11] H. G. Akhavan and D. Mirshekar-Syahkal, “Approximate model for microstrip fed slot antennas,” *Electron. Lett.*, vol. 30, no. 23, pp. 1902–1903, Nov. 1994.

[12] *HP Momentum*, Hewlett-Packard, Santa Rosa, CA.

[13] R. F. Harrington, *Time Harmonic Electromagnetic Fields.* New York: McGraw-Hill, 1961.

[14] D. R. Rhodes, “On a fundamental principle in the theory of planar antennas,” *Proc. IEEE*, vol. 52, pp. 1013–1021, Sept. 1964.

[15] T. Itoh, “Spectral domain immittance approach for dispersion characteristics of generalized printed transmission lines,” *IEEE Trans. Microwave Theory Tech.*, vol. MTT-28, pp. 733–736, July 1980.

[16] A. K. Bhattacharyya and R. Garg, “Effect of substrate on the efficiency of an arbitrarily shaped microstrip patch antenna,” *IEEE Trans. Antennas Propagat.*, vol. AP-34, pp. 1181–1188, Oct. 1986.

[17] K. C. Gupta, R. Garg, I. Bahl, and P. Bhartia, *Microstrip Lines and Slotlines*, 2nd ed. Dedham, MA: Artech House, 1996.

[18] R. E. Collin, *Foundations for Microwave Engineering*, 2nd ed. New York: McGraw-Hill, 1992.

Jeong Phill Kim (M'98) was born in Cheju, Korea, on November 2, 1964. He received the B.S. degree in electronic engineering from Seoul National University, Seoul, Korea, in 1988, and the M.S. and Ph.D. degrees in electrical engineering from Pohang University of Science and Technology, Pohang, Korea, in 1990 and 1998, respectively.

Since 1990, he has been with the Research and Development Center at LG Precision Co., Ltd., Yongin, Kyunggi, Korea, where he has been involved with the design of various radar transmitters and receivers. His research interests include microstrip circuits and antennas, dielectric resonator antennas, numerical modeling and analysis, and microwave measurements.

Wee Sang Park (M'89) was born in Korea, in 1952. He received the B.S. degree in electronic engineering from Seoul National University, Korea, in 1974, and the M.S. and Ph.D. degrees in electrical engineering from the University of Wisconsin, Madison, in 1982 and 1986, respectively.

From 1986 to 1988, he taught at Wichita State University, Wichita, KS, as a Visiting Assistant Professor. He joined Pohang University of Science and Technology, Korea, in 1988 and is currently an Associate Professor in the Department of Electronic and Electrical Engineering. Since 1995, he has been Director of the Antenna Laboratory of Microwave Application Research Center, POSTECH. In 1997, he spent a one-year sabbatical leave at the Bioelectromagnetics Laboratory, University of Utah, Salt Lake City. He has been involved in electromagnetics, microwave, and antenna engineering for the last 16 years. He is currently an Associate Editor of the Korea Electromagnetic Engineering Society. He has authored and coauthored more than 80 technical journal articles and conference papers. He has made contributions to the developments of material constant measurement methods using coaxial line, cylindrical cavity, and dielectric resonator. He established network models for microstrip slot or slotline for the design of microstrip-patch and flared-notch antennas and multilayer microstrip circuit. He developed phase shifters with ferrite meander lines and p-i-n diodes. With these components, he developed microstrip phased array antennas and tested them with a near-field probe. He also developed FDTD codes to simulate the interaction between cellular phone and the human head and to analyze various microstrip discontinuities. His recent interest includes the measurement of SAR for portable phones and development of a bone equivalent material for human phantom.

Dr. Park is a member of the IEEE Microwave Theory and Techniques and Antennas and Propagation Societies. He is also a member of the Institute of Electronics Engineers of Korea.